Ceramics-Silikáty 65 (4), 354-362 (2021)
www.ceramics-silikaty.cz doi: 10.13168/cs.2021.0037

PREPARATION OF HYDROGEL PARAFFIN MICROCAPSULES AND ITS EFFECT ON THE SHRINKAGE OF CEMENT MORTARS

XIAO-DONG JIAO*,**,***, #JIAN-PING XIONG*,**,***, YANG-PENG ZHANG*,**,***, BI-YUN LI*,**,***, ZHENG-ZHUAN XIE*,**,***,WEI-DONG LIU*,**,***, MING-ZHU FENG*,**,***

*Guangxi Key Lab of Road Structure and Materials, Nanning 530007, China
**Research and Development Center on Technologies, Materials and Equipment of High Grade Highway Construction and Maintenance Ministry of Transport, Nanning 530007, China
***Guangxi Transportation Science and Technology Group Co., Ltd, Nanning 530007, China

#E-mail: jxd991164424@163.com

Submitted July 25, 2021; accepted September 16, 2021

Keywords: Hydrogel paraffin microcapsules, Cement-based materials, Shrinkage properties, Cement hydration, Pore structure

In an attempt to solve the uncontrollable water absorption of a superabsorbent polymer (SAP), microcapsules (MPCP), with calcium alginate and paraffin powder as the main raw materials, were prepared. The structure and water absorption properties of the MPCP was characterised and its influence on the shrinkage performance of a cement mortar was studied. The shrinkage-reducing mechanism of the MPCP was analysed through the heat of cement hydration, pore structure and relative humidity (RH) of the cement mortar. The results show that the MPCP particles are based on a calcium alginate network skeleton structure with a paraffin wax filling the round particles in the skeleton cracks, where its content determines the water absorption of the MPCP. The MPCP exhibited a good internal curing effect. The internal RH of the mortar containing the pre-absorbed MPCP basically changed as much as that containing the pre-absorbed SAP. The shrinkage of the MPCP-containing mortar reduced by more than 8 % compared with the SAP-containing mortar after 7 days. The reason was that the MPCP absorbed the heat of the cement hydration and reduced the shrinkage caused by the excessive heat of the early cement hydration. In addition, because the water absorption of the MPCP is controllable, the MPCP exhibits little effect on the pore structure of cement-based materials. Therefore, the compressive strength of the cement mortar with the pre-absorbed MPCP content is 39 times that of the pre-absorbed SAP, which was only 2.3 MPa lower than that of the corresponding SAP-containing cement mortar.

INTRODUCTION

With the development of modern technologies and admixtures, the water-to-binder ratio (w/b) of cement-based materials is constantly decreasing. For example, the water-to-binder ratio in the design of high-strength and high-performance concrete is generally less than 0.38, and some other high-performance concretes have ratios below 0.2. A decreased w/b ratio leads to a reduced internal pore moisture content, which, in turn, increases the internal stress of the concrete pores, resulting in concrete shrinkage and cracking [1-3]. Among the causes of cracks in the structures of cement-based materials, 80 % of the non-load cracks are caused by the concrete materials themselves. The main sources of these non-load stresses are the early temperature shrinkage, autogenous shrinkage, and drying shrinkage of cement-based materials [4-5].

The early cracking of cement-based materials results from the gradual consumption of the internal moisture of the structures as the cement hydrates, leading to an increase in the negative pressure of the capillary pores, thereby causing the pores to collapse. In addition, cement hydration proceeds quickly after mixing of cement-based materials, causing the release of large amounts of heat, resulting in large temperature differences between the inner and the outer sections of cement-based materials. This ultimately causes volume shrinkages [6]. These changes are eventually reflected by the macroscopic volume reduction of the cement-based materials. Therefore, restraining the shrinkage and preventing cracks in cement-based materials is of great significance to their engineering safety and durability. At present, one of the main technologies for reducing shrinkage in cement-based materials is an internal curing technology, where an internal curing material prolongs the hydration of the cement by releasing water when the moisture inside the cement-based materials decreases, thereby reducing the internal pore pressure and restricting the pore collapse. Furthermore, the water released by the internal curing material can also promote the hydration of unhydrated cement, and enhance the performance of the transition zone of the concrete interface. Among the commonly used internal curing materials, superabsorbent polymers (SAPs) are the most widely used.

A SAP is a polymer hydrogel with a three-dimensional network structure. Its molecular chain contains a large number of strong hydrophilic groups, and its water absorption rate can reach dozens of times its own mass. The research of Pang [7] and Kong [8] et al. showed that cement-based materials mixed with pre-absorbent SAP have a good shrinkage reduction effect. Cracyc B [9] et al. added non-absorbent SAP to a low water-cement ratio concrete, and found that the concrete displayed good shrinkage after the addition of an extra 30 - 50 kg of water per cubic meter. However, the uncontrollable water absorption of SAP can adversely affect the working performances and mechanical properties of cement-based materials [10-12]. Yao [13] et al. reported that SAP reduces the compressive strength of cement-based composites by about 15 %, while Jenson [14] et al. recorded a 15 % to 20 % reduction in the compressive strength of cement mortars mixed with SAP during standard curing. Furthermore, Kong et al. [15] reported the ease in the production of large pores in SAPs after its water-releasing function in cement-based materials, with most pores being irregular and in the range of 200 ~ 600 μm. Using an X-ray microtomography three-dimensional analysis, Lura [16] found significant differences between the pore structure of a SAP-containing mortar with that of an ordinary mortar, with the ordinary mortar having pores of several microns compared to the several hundred microns of the SAP mortar.

In view of the challenges associated with controlling the moisture absorption and release of SAP which negatively impacts the fluidity and mechanical properties of concretes, this study became necessary. Herein, the orifice coagulation bath method was used to prepare microcapsules (MPCP) with a calcium alginate hydrogel and paraffin wax as the main materials towards achieving controllable water absorption and release performances, and to address the uncontrollable water absorption challenges of SAP. In addition, paraffin wax is a hydrophobic phase change material having a good temperature control effect. Therefore, it was expected that the MPCP will exhibit an improved temperature control effect, thereby reducing the temperature shrinkage of cement-based materials, while achieving an internal curing effect. In general, this study investigates the impact of MPCPs on the shrinkage of a cement mortar, while exploring the possible internal factors influencing its effects on the shrinkage by using the heat of the cement hydration and the change in the relative humidity (RH).

EXPERIMENTAL

Materials

Sodium alginate (SA), paraffin powder, and anhydrous calcium chloride were supplied by the West Asia Reagent Company. Tween 60 (TB19613), Span 60 (S818142) and carbon tetrachloride were obtained from Macleans. The SAP, with a particle size not greater than 0.45 mm, was supplied by Beijing Hanlisen New Technology Co., Ltd. P.O 42.5R grade ordinary Portland cement was obtained from the Sichuan Esheng Cement Group. The oxide composition of the cement and mineral composition of the clinker minerals are reported in Table 1. The standard sand used in this investigation was provided by Chengdu Shanli Mining Co., Ltd., and its particle size distribution is shown in Table 2. The ZY13 water reducing agent, with a solid content of 40 % and a water reducing rate of 30 %, was produced by China Construction West Construction New Material Technology Co., Ltd. The deionised water and saturated lime water used in the experiment were made in the laboratory.

Table 2. ISO standard sand particle size distribution.

Sieve size (mm)	Accumulated sieve residue (%)	Sieve size (mm)	Accumulated residue (%)
2.0	0	0.5	67.5
1.6	7 ± 5	0.16	87 ± 5
1.0	33 ± 5	0.08	99 ± 1

Microcapsule preparation and performance

Preparation of the MPCP

The SAP and deionised water with a mass ratio of 1:60 were poured into a thermostat at 65 °C. After an even mixture, the paraffin powder and paraffin emulsifier (Span 60 and Tween 60 in a 1:1 mass ratio) were added, with the amount of the emulsifier being added at about 35 % to 40 % of the mass of the paraffin wax powder. The mixture was fully stirred for 3 ~ 4 h to obtain a milky white liquid, followed by the dropwise addition of an anhydrous calcium chloride solution with a mass concentration of 8 % by means of a syringe. The resulting solution was left to stand for 3 ~ 5 h to obtain the MPCP.

The microstructure of the MPCP

The structure and microstructure of the MPCP was characterised by infrared spectroscopy and a scanning electron microscope (SEM), respectively. For the infrared

Table 1. Chemical and mineral compositions of the reference cement.

Composition	SiO_2	Al_2O_3	Fe_2O_3	CaO	MgO	SO_3	Na_2O	f-CaO	C_3S	C_2S	C_3A	C_4AF
Cement / %	22.93	4.29	2.89	66.23	1.92	0.35	0.70	0.64	58.78	21.38	6.49	8.77

spectroscopic analysis, the prepared MPCP was dried in a vacuum at 45 °C for 12 hours, and then a certain mass of the solid sample with KBr was mixed and pressed into a sheet. A VVERTEX 70 infrared spectrometer (German Brooks Company) was used to test the MPCP at room temperature, and the spectrum range was measured from 4000 cm^{-1} to 400 cm^{-1}. In addition, the dried MPCP was repeatedly rinsed with perchloroethylene to remove the core material. The capsules, from which the core material was removed, were dried and cut into thin slices, adhered to the sample stage with conductive glue, and sprayed with gold to investigate the microstructure of the sample under different magnifications using a Merlin scanning electron microscope (Zeiss, Germany).

The content of the MPCP core material

The dried weight of the MPCP was taken as m_0 g. The material was then ground to ensure the complete dispersion of the paraffin powder, and washed 3 - 5 times with acetone before drying. The dried microcapsules were weighed and recorded as m_t g. Finally, the content of the MPCP core material was calculated based on Equation 1, as shown:

$$C = \frac{m_0 - m_t}{m_0} \times 100\ \% \qquad (1)$$

where C is the microcapsule core material content (%), m_0 is the mass of the microcapsule (g), and m_t is the mass of the microcapsule after the core removal (g).

The water absorption and release performance of the MPCP:

The dried MPCP was added into saturated lime water and its change in quality was monitored every 12 hours until no obvious change was observed. Equation 2 was then used to calculate the water absorption of the MPCP.

$$A = \frac{M_t - M_0}{M_t} \times 100\ \% \qquad (2)$$

where A is the water absorption rate of the microcapsule core material (%), M_0 is the mass of the microcapsule before the water absorption (g), and M_t is the mass of the microcapsule after the water absorption (g).

The water release performance of the microcapsules was investigated by placing the MPCP in an environment with a temperature of 20 ± 2 °C and relative humidity (RH) of 50 ± 5 % after the water absorption to monitor its quantity variation.

The influence of the MPCP on the properties of cement-based materials

The shrinkage of mortar

The mortar containing the MPCP was placed in a 25 × 25 × 280 mm prismatic triple mould and cured for 24 ± 2 h at room temperature. Afterwards, the demoulded mortar was fixed to a wireless cement-based deformation measuring instrument. The temperature of the mortar shrinkage test was controlled at 20 ± 2 ℃, with a RH of 55 ± 5 %, and the mortar shrinkage was calculated according to Equation 3.

$$K_n = \frac{(L_0 - L_n) \times 100}{250} \qquad (3)$$

where K_n is the shrinkage of the cement mortar specimens in n days (%), L_0 is the initial test length (mm), L_n is the test length after n days (mm), and 250 is the effective length of the mortar specimen (in mm).

Cement hydration test: The cement, deionised water and MPCP were weighed under a certain water-cement (W/C) ratio, and transferred into a sample bottle, which was placed in a pre-heated TAM AIR-08 multi-channel isothermal calorimeter. The heat of the hydration of the cement paste was then tested over time after quickly stirring for 30 seconds.

Internal relative humidity: The paraffin wax was evenly applied on a 150 × 150 × 150 mm mould preceding the addition of the mixed cement mortar into the mould. A humidity sensor was inserted in the middle of the mortar. After 4 hours of mortar formation, the upper layer of the mortar was sealed with paraffin wax. Then the RH of the slurry was tested in an environment controlled at 20 ± 2 °C and 50 ± 5 % relative humidity.

The compressive strength of mortar: The mixed cement mortar was moulded in a 25 × 25 × 160 mm triple mould, and then demoulded after curing for 24 hours at room temperature. The prisms were then cured for 7 and 28 days in an environment controlled at 20 ± 2 ℃, RH = = 50 ± 5 %. The strength of the cement mortar was tested according to the Chinese standard GB/T 17971-1999 “Method for Testing the Strength of Cement Mortar Sand (ISO)” [18].

Mercury intrusion porosimetry (MIP) experiment: The prepared paste sample was cured for 7 days in an environment having a temperature of 20 ± 2 ℃ and RH of 55 ± 5 %. The sample was then crushed into small particles of 3 - 5 mm in diameter, followed by the termination of the hydration with absolute ethanol for 24 h. The crushed particles were dried in a vacuum drying oven at a temperature of 40 °C for 24 h. Then the pore structures and changes in the pore diameter of the slurry were tested using an Auto Pore IV mercury porosimeter, manufactured in the United States.

RESULTS AND DISCUSSION

The structure of the microcapsules

Figure 1 shows the infrared spectra of the MPCP, paraffin powder and calcium alginate. From the figure, the functional groups in the paraffin wax are a benzene ring, a C=O bond, a C–O–C bond, and an OH vibration bond. In the infrared spectrum of the paraffin powder, the peak at 2900 cm^{-1} is attributed to the asymmetric stretching vibration of $–CH_3$, while the peaks at

1693 cm^{-1}, 1475 cm^{-1}, and 939 cm^{-1} were assigned to the C=O stretching vibration peak, C=C vibration peak of the benzene ring, and the C–O–C vibration stretching, respectively. These peaks were also characterised in the MPCP, indicating the presence of paraffin in the MPCP sample. The infrared spectrum of the calcium alginate displayed an O–H stretching vibration peak at 3340 cm^{-1} and a C=O stretching vibration peak at 1650 cm^{-1}. These peaks were reflected in the mid-infrared spectrum of the MPCP, indicating the presence of calcium alginate in the MPCP. The infrared spectrograms show that the main components of the MPCP were sodium alginate and paraffin wax.

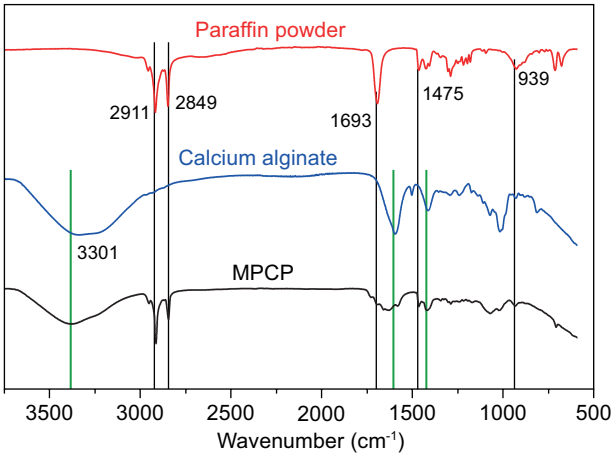

Figure 1. The FTIR spectra of the MPCP, paraffin powder and calcium alginate.

Figure 2, which shows the SEM image of the MPCP, reveals that it is a hollow capsule with a diameter of about 1.5 mm and possessing a membrane. Energy-dispersive X-ray spectroscopy (EDS) measurements were performed on the inner and outer layers of the MPCP, and it was found that the outer layer contained a higher amount of Ca than the inner layer. This shows that the outer layer of the MPCP was composed of more of the calcium alginate gel, while the inner layer mainly contained the paraffin powder. On magnification of the outer layer, it was observed that the calcium alginate had a honeycomb structure, with paraffin powder occupying some of its voids. Combining the results from the infrared spectroscopy and SEM analysis, it is clear that the MPCP is a hollow spherical capsule with calcium alginate-dominated outer shell and paraffin powder-dominated inner layer.

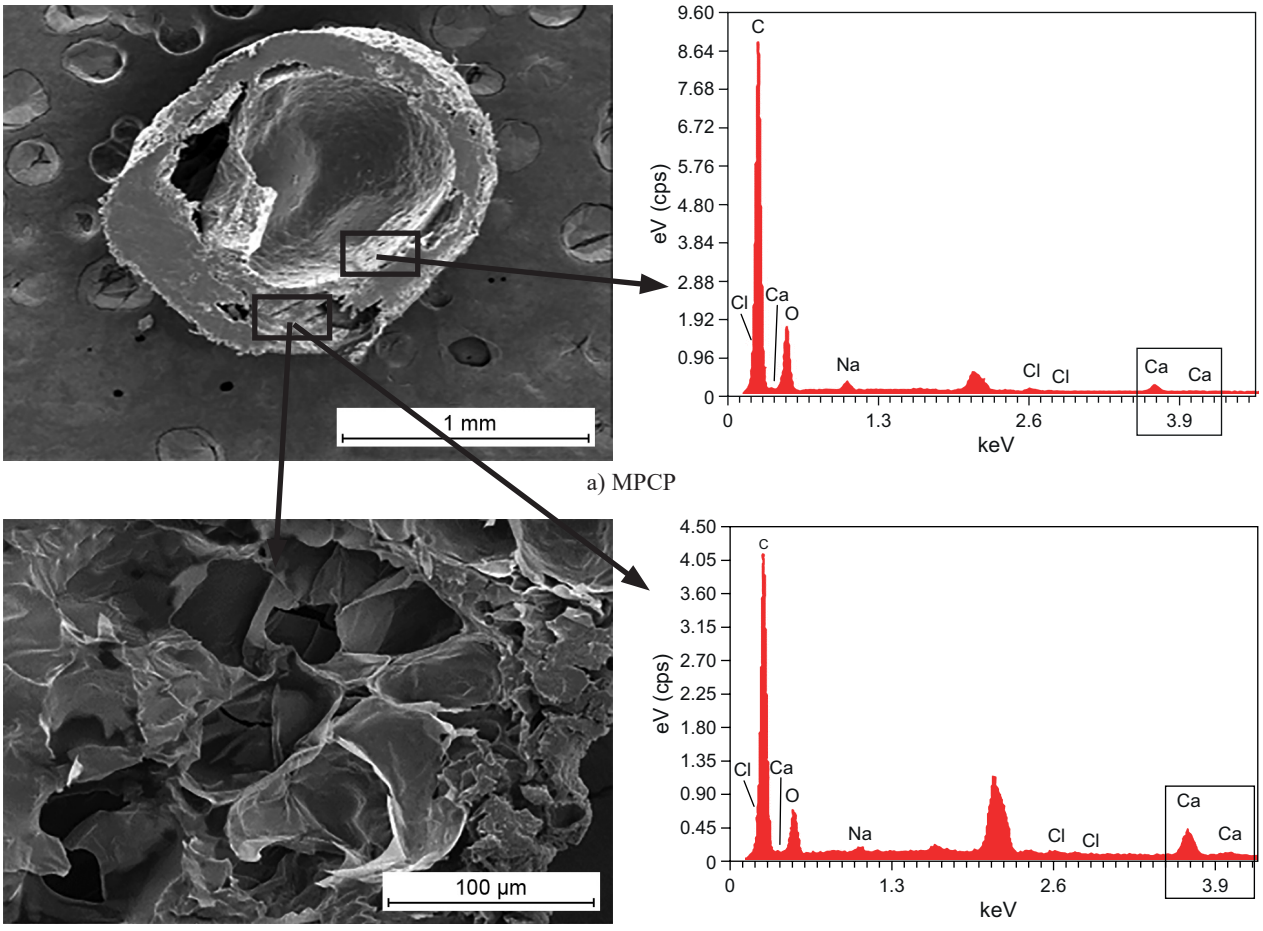

Figure 2. SEM micrographs of the MPCP.

Microcapsule performance

Table 3 shows the MPCP with different core material contents prepared under different sodium alginate and paraffin powder ratios, and the water absorption rates of the MPCP in the saturated lime water. It can be seen from Table 2 that with an increasing paraffin wax content, the MPCP core material content increased and its water absorption in the saturated lime water decreased. The MPCP core material filled the pores of the calcium alginate. When the content of the core material increased, the porosity of the calcium alginate decreased due to the occupation of the core material, resulting in a decrease in the water absorption rate of the calcium alginate. Therefore, the water absorption rate of the MPCP can be adjusted by the ratio of the raw materials to achieve different water absorption rates.

Table 3. Paraffin powder content and water absorption rates of the MPCP under different raw material ratios.

m_{SA} : $m_{paraffin\ powder}$	2	3	4
Paraffin powder content (%)	34.1	46.7	67.5
Water absorption rate (%)	71.3	63.5	49.8

Figure 3 shows the water release capacity of the MPCP with the different core material contents after absorbing water to saturation at 20 ± 2 °C and 50 ± 5 % RH. To evaluate the water release capacity of the MPCP, the test results with the pre-absorbed SAP were used as the comparison, and the SAP absorbed water 25 times its own mass. As seen in Figure 3, the MPCP exhibited a slow water release capacity in a drier environment. The MPCP and SAP showed equivalent water losses up to 7 h, but with time, the water loss capacity of the MPCP became lower than that of SAP. This is because MPCP has a lower water absorption rate than SAP. Its water loss reaches a level where the water in the internal structures does not easily flow out. This means that while the MPCP has special water absorption and release abilities, it also exhibits some basic internal maintenance requirements.

The shrinkage of the cement mortar

An MPCP with a water absorption rate of 63.5 % was used for the shrinkage test of the cement mortar. In order to study the impact of the MPCP on the shrinkage performance of the cement mortar, the following three water-cement ratios were employed [2]: the effective water-cement ratio (We/C) (ratio of the cement mortar mixing water to the cement quantity); the internal curing water-cement ratio (W_i/C) (ratio of the additional water introduced by the MC and SAP to the cement quantity); and the total water-cement ratio (W_t/C) (ratio of the sum of the We/C and W_i/C). Table 4 shows the ratio of the cement mortar, and the mixing amount of MPCP and SAP after the water absorption is determined according to its internal curing W_m/C. The amount of water reducing agent (PCE) was enough to control the initial fluidity of the cement mortar to 140 ~ 150 mm.

Figure 4 illustrates the effect of adding the MPCP (with a water absorption rate of 63.5 %) and SAP (with a pre-absorption rate 25 times its mass) on the shrinkage

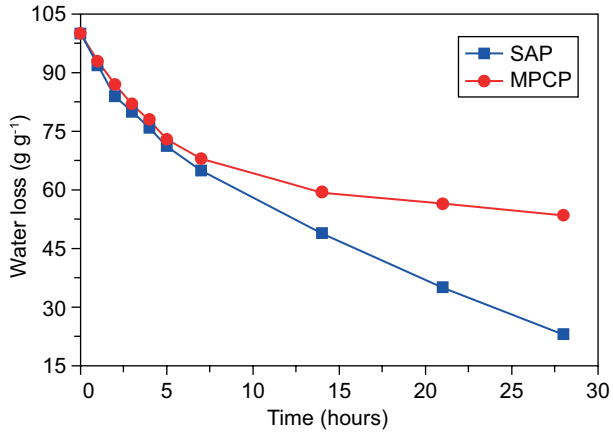

Figure 3. The drying moisture loss curve of the pre-absorbed MPCP and SAP.

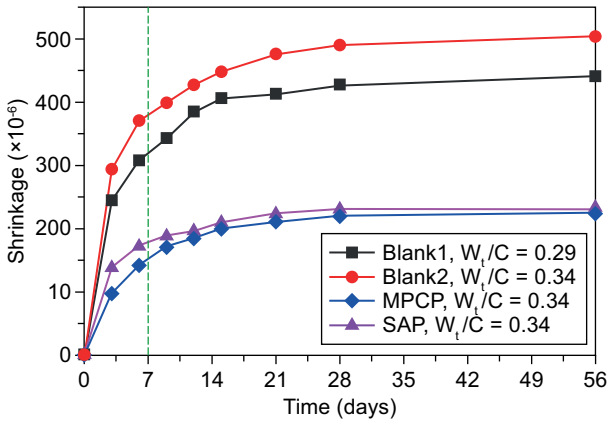

Figure 4. Shrinkage properties of the hardened cement mortar.

Table 4. Design of the cement mortar mix ratio.

Samples	W_e/C	W_m/C	W_t/C	Mass (g)				
				MPCP	SAP	Cement	Standard sand	Admixtures
Blank1	0.29	–	0.29	–	–	450	1350	12
Blank2	0.34	/	0.34	–	–	450	1350	8.5
MPCP	0.29	0.05	0.34	20.4	–	450	1350	10.8
SAP	0.29	0.05	0.34	–	0.52	450	1350	10.4

performance of the cement mortars. The figure shows that each sample exhibited large early shrinkage, which eventually decreased after 14 days. This was due to the effect of the hydration shrinkage (0 ~ 3 d), self-drying shrinkage (1 - 14 d) and drying shrinkage (> 7 d). The autogenous shrinkage of the mortar basically ended by the 14th day, and this is evident by the slow shrinkage rate after 14 d. The rate of mortar shrinkage increased with an increase in the W/C ratio for the Blank group. This can be explained by the increase in the connecting pores of the cement paste after increasing the W/C ratio, which enhanced the flow of water from the pores in the mortar, resulting in an increase in the mortar shrinkage [9, 19].

In comparing the curves of Blank1, SAP and MPCP with the same W_e/C, it is observed that the MPCP-containing mortar exhibited the same shrinkage effect as the SAP one after 56 days, but the early shrinkage reducing effect of the mortar with the MPCP was more obvious than that of the SAP-containing sample. In comparison with Blank1 at 7 days, the MPCP reduced the mortar shrinkage by 61.3 %, while the SAP reduced the mortar shrinkage by 52.6 %. Comparing the curves of Blank2, MPCP and SAP with a W_t/C ratio of 0.34, the shrinkage of the MPCP mortar was reduced by 55.4 % compared with Blank2 at 14 days, while it reduced by 53.1 % for the SAP sample. This shows that the pre-absorbed MPCP had a good shrinkage reduction effect, and the early shrinkage reduction effect of the mortar containing MPCP was better than that of SAP. This may be due to the lower water absorption of MPCP than the SAP. In the cement mortar system, the early water release ability of the MPCP was weaker than that of SAP, and the pores formed after the water release were smaller. In addition, the MPCP may have exhibited a better temperature regulation ability in the early stage of the cement hydration, causing a superior shrinkage reduction effect of the MPCP-containing mortar compared with the SAP-containing mortar. This observation requires further investigation.

Analysis of the microcapsules reducing shrinkage

Relative humidity inside the cement mortar

Figure 5 shows the dependence of the RH of the mortar samples after mixing with the pre-absorbent MPCP over time. It can be seen from Figure 5 that the RH of each sample gradually decreased with time, mainly due to the water consumption during the cement hydration. In comparing the Blank2, MPCP- and SAP-containing samples with a W_t/C ratio = 0.34, the RH of the Blank2 sample showed the highest variation with a value of 86.7 % after curing 336 hours, while the RH also decreased with an increasing curing time for the MPCP- and SAP-containing samples, but with very small variations when compared with Blank2. They maintained 95 % RH through the 336 hours of the curing duration.

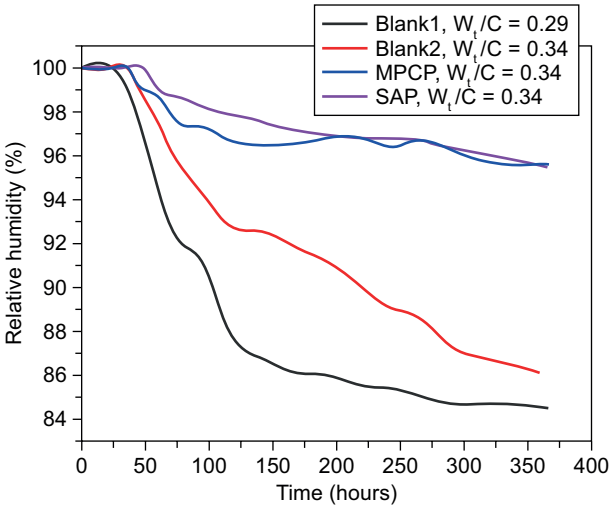

Figure 5. The relative humidity of the cement mortars.

The existing research results show that the SAP is unable to release the stored water in the initial stages of cement hydration. As the RH inside the mortar decreases, the SAP releases the internal water to fill the internal pores of the cement-based material, thereby reducing the shrinkage caused by the decrease in the capillary pore moisture. It can be seen from Figure 5 that the internal RH change of the MPCP-containing mortar was basically the same as that of SAP sample. This shows that the pre-absorbed MPCP had the same internal humidity adjustment ability as SAP for the cement-based materials, and had a good internal curing and shrinking reducing effect.

Heat of hydration of cement

The MPCP is composed of calcium alginate and paraffin powder, and paraffin powder as a phase change material has good temperature control ability [12, 13]. Therefore, the effect of the MPCP on the heat of hydration of the cement was tested. The W/C ratio, MPCP and SAP content of the cement hydration test were consistent with Table 3 (without the PCE), and the effect of MPCP on the heat of cement hydration is shown in Figure 6. While Figure 6a shows the hydration heat release rate, Figure 6b shows the cumulative heat release.

A comparative analysis of the Blank1 and Blank2 samples shows that the Blank2 sample, with a larger W_t/C ratio, had its peak of hydration exotherm during the accelerated period of cement hydration appear before that of Blank1, and it exhibited an increased hydration exotherm rate. Moreover, Figure 6b shows that the Blank2 sample had the highest heat of hydration. The reason was that the Blank2 sample with the increasing free water content increased the contact area of the cement particles with the free water, which promoted the cement hydration and increased the amount of heat released in the early stage of the cement hydration. This is an antagonistic effect to the early shrinkage reduction of cement-based materials.

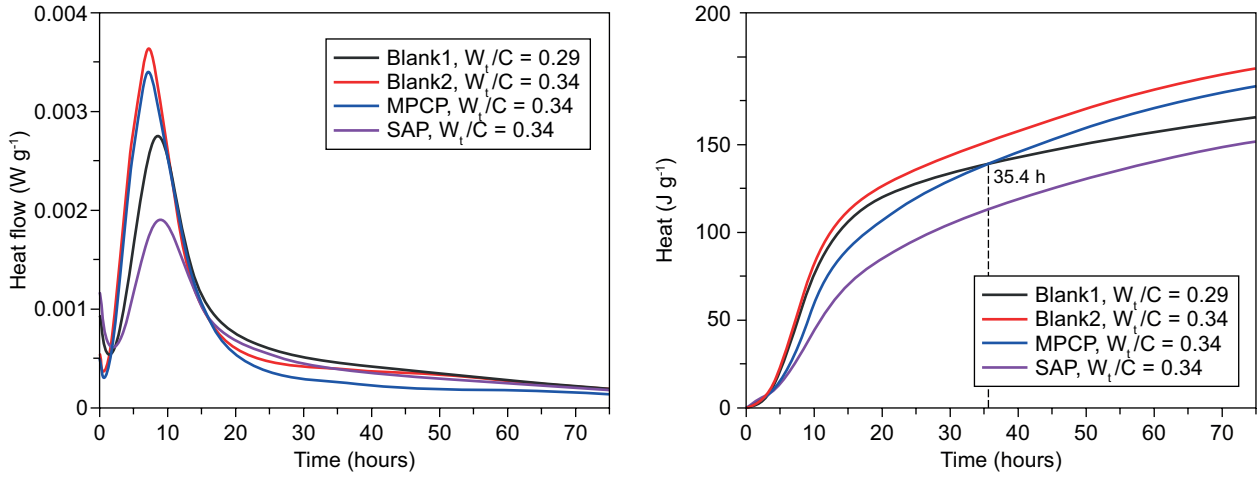

a) Hydration heat release rate

b) Cumulative heat release

Figure 6. Calorimetry curves of the cement pastes with the MPCP and SAP.

It can be seen from Figure 6a that the MPCP reduced the hydration heat release rate at the peak position compared with Blank1 and SAP with the same W_e/C ratio, and also displayed a hydration delaying effect. Also, Figure 6b shows that the cumulative heat release of the MPCP sample was the smallest at 72 hours. This shows that, in the early stage of cement hydration, the paraffin powder in the MPCP had a good temperature control ability, which effectively slowed down the cement hydration process.

In comparing the SAP and Blank1 samples, it is obvious that the SAP increased the cement hydration heat release rate at the peak period, and, after hydration for 35.5 hours, the SAP had a higher heat of hydration than Blank1. This means that the SAP did not participate in the initial stage of the cement hydration. As the cement hydration reaction consumes water, the internal RH of the cement-based material reduces, and the SAP releases internal water to participate in the cement hydration.

In comparing the Blank2, MPCP and SAP samples with the same W_t/C ratio, both the MPCP and SAP slowed down the peak of cement hydration and cumulative heat release. This is because the water stored in the MPCP and SAP did not take part in the cement hydration at the beginning, but as the internal moisture of the pastes decreased, the MPCP and SAP released their internal moisture and participated in the cement hydration, which accelerated the rate of the heat release from the hydration reaction. Furthermore, the heat-absorbing property of the MPCP ensured that the final heat release was reduced, which resulted in a reductio in the shrinkage caused by the heat release from the hydration of the cement-based materials.

Pore structure

Bensted et al. [20] reported that pores between 10 to 100 nm have an important influence on the autogenous shrinkage, drying shrinkage and creep of cement-based materials. For this reason, the cement pastes were prepared according to the ratio shown in Table 2, and their pore structures after 14 days of curing were tested and presented in Figure 7. The figure shows the effect of the MPCP addition on the pore structure of the cement pastes after hardening for 14 days, where Figure 7a describes the cumulative mercury intrusion, and Figure 7b displays the pore size distribution, while Table 4 presents the pore size distribution data.

It can be seen from Figure. 7a that the cumulative intrusion in the pastes increased with an increase in the W/C ratio. This is because the pores in the pastes increased as the W/C ratio increased, resulting in an increase in the amount of cumulative intrusion. In comparing the samples with a W_t/C ratio of 0.34, it was found that the cumulative intrusions of the Blank2 and SAP samples were basically the same. The MPCP sample had the largest cumulative intrusion, with its amount being 39 times higher than that in the SAP sample. After the release of internal moisture, there were more pores in the MPCP sample than the SAP sample.

Table 5. Pore structure parameters of the cement mortars.

Mixture	Cumulative intrusion ($ml \cdot g^{-1}$)	Porosity (%)	Pore size distribution (%)			
			< 10 nm	10 ~ 100 nm	100 ~ 1000 nm	> 1000 nm
Blank1	0.0493	10.9446	4.86	51.87	26.74	16.53
Blank2	0.0713	15.0492	5.22	62.35	15.79	16.64
MPCP	0.0804	16.7330	5.34	46.14	22.40	26.12
SAP	0.0729	15.4636	5.46	44.17	12.87	37.50

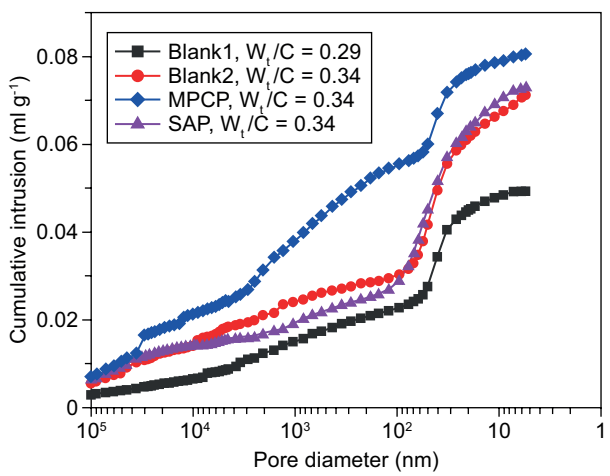

a) Total pore volume versus pore size

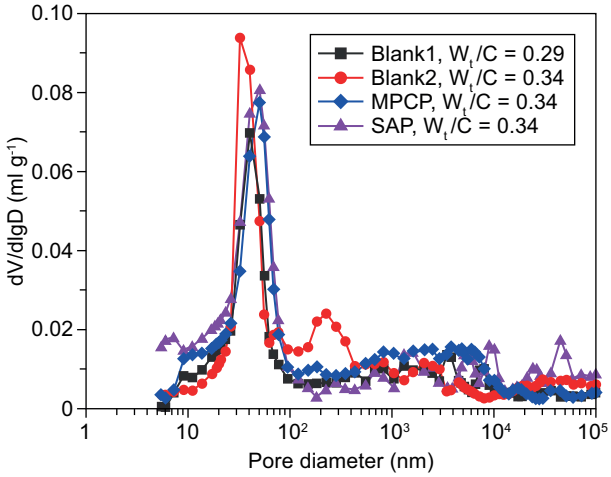

b) Derivative of the pore volume versus pore size

Figure 7. Results of the MIP experiment.

It can be seen from Figure 7b that each sample exhibited peaks within 10 ~ 100 nm. Additionally, the Blank2 sample had an obvious peak within 100 ~ 1000 nm, while the other samples basically showed no peak within this range. All the samples also displayed smaller peaks in the 1000 ~ 10 000 nm range. For the SAP-containing sample, a larger peak appeared after > 10 000 nm. Combining Figure 7b and Table 4, it is clear that without internal curing materials (Blank samples), the pore size distribution within 10 ~ 100 nm increased with an increase in the W/C ratio, which tends to cause shrinkage of cement-based materials. For the SAP-containing samples, the pore diameter within 10 ~ 100 nm was smaller than that of Blank2 with the same W_t/C ratio, which is beneficial for shrinkage reduction. The pore size of the MPCP-containing sample at 10 ~ 100 nm was smaller than those of the Blank group, and had the same change trend as the SAP-containing sample. Therefore, the shrinkage reduction of MPCP sample was also reflected in the adjustment of the pore structure.

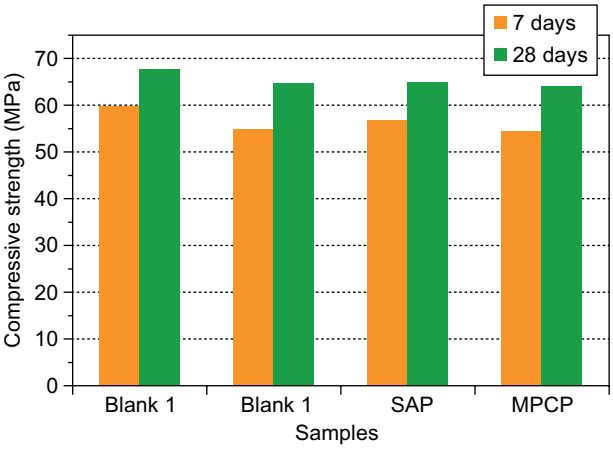

Figure 8. The compressive strength of the different cement mortars.

The large increase in the pore size of the SAP sample > 1000 nm can be explained by the significant reduction in the volume of the pre-absorbed SAP gel particles after the water loss. The pore diameter for the MPCP sample > 1000 nm was 11.38 % smaller than that of the SAP sample, meaning that a fewer number of pores were produced after the water loss from the MPCP sample. This is because MPCP has a small water absorption rate, and its volume does not change significantly after the water absorption and release.

Mechanical properties

Figure. 8 shows the effect of the MPCP on the compressive strength of the hardened mortar samples. Comparatively for the samples with the same W_t/C ratio, the compressive strengths of the MPCP sample were equivalent to those of the Blank2 sample, and slightly lower than those of the SAP sample. In the cement mortar preparation, the amount of added MPCP was 39 times than that of the SAP. This is responsible for the larger porosity of the MPCP sample, hence the slightly lower compressive strength. This means that the MPCP has a lower influence on the strength than the SAP. This can be better explained by the smaller water absorption rate of the MPCP, leading to smaller pores after the water loss (as previously described in section 3.4.3). This resultantly weakens its influence on the strength of cement-based materials. Therefore, in the actual application process, it is necessary to adjust the water absorption rate of the MPCP so as to reduce its dosage to an optimal level that permits the best internal curing and mechanical properties.

CONCLUSIONS

Calcium alginate-paraffin hydrogel microcapsules were prepared and characterised, and their water absorption under different raw material ratios, as well

as their influence on the shrinkage performance of the cement mortar, were tested. The accompanying results were exhaustively discussed and the main conclusions obtained are as follows:

- MPCP is a spherical capsule with a paraffin powder-dominated inner layer and an outer layer largely composed of calcium alginate gel. Calcium alginate has a honeycomb shape with parts of its voids filled with paraffin powder, leaving the unfilled voids as water storage locations. Therefore, the water absorption rate of the MPCP can be controlled by adjusting the ratio of the raw materials.
- Just like SAP, MPCP exhibited water absorption, water release, and internal curing effects, which were responsible for its effective shrinkage-reduction effects on the cement-based materials. In addition, the MPCP displayed a cement hydration delay behaviour, which was beneficial for the reduction of the shrinkage due to the cement hydration.
- In comparison with SAP, after the internal moisture release by the pre-absorbed MPCP in the cement mortar, the numbers of macrospores in the paste were reduced, and this weakened the compressive strength of the cement mortar.

Acknowledgment:

The authors gratefully acknowledge the financial support provided by the Scientific Research and Technology Development Program of Guangxi (AC19050010, AB17292032 and AB19259008) and Natural Science Foundation of Guangxi Province (2018GXNSFAA281339).

REFERENCE:

1. Dong F Y., Zhen S S., Song M C., et al. (2018): Research progress of high performance concrete II: durability and life prediction model. *Materials Reports, 32*(03), 163-169, 176. doi: 10.11896/j.issn.1005-023X.2018.03.021.
2. Wang W Z., Shen A Q., He Z M., et al.(2021): Mechanism and erosion resistance of internally cured concrete including super absorbent polymers against coupled effects of acid rain and fatigue load. *Construction and Building Materials, 290*, doi:10.1016/J.CONBUILDMAT.2021.123252.
3. Jenson O M., Hansen P F., (2002): Water-entrained cement-based materials: II Implement and experimental results. *Cement and Concrete Research, 32*(6), 973-978. doi: 10.1016/S0008-8846(02)00737-8.
4. Wang D H., Shi C J., Wu L M. (2016): Research and application of ultra-high performance concrete (UHPC) in China. *Bulletin of the Chinese Ceramic Society, 35*(1), 141-149. doi: 10.16552/j.cnki.issn1001-1625.2016.01.026.
5. Wan G P., Li H J., Huang J M. (2012): Review of research progress on concrete internal curing technology. *Concrete* (in chinese), 51-54, 66. doi:CNKI:SUN:HLTF.0.2012-07-018.

[6] Miu C W (2019): Early-age deformation and shrinkage crack control of modern concrete. Science Press. *Journal of Xuzhou Institute of Technology* (in Chinese) *129*(03), 7-14. doi: CNKI:SUN:OXZG.0.2018-03-001.

7. Pang L F., Ruan S Y., Cai Y T. (2011): Effects of internal curing by super absorbent polymer on shrinkage of concrete. *Key Engineering Materials, 477,* 200-204. doi: 10.4028/www.scientific.net/KEM.477.200.
8. Kong X M., Zhen Z L. (2014): Investigation on the shrinkage-reducing effect of super-absorbent polymer in high strength concrete and its mechanism. *Journal of Building Materials.* (4), 559-565. doi: 10.3969/j.issn.1007-9629.2014.04.001.
9. Craeye B., Geirnaert M., Schutter G D. (2011): Super absorbing polymers as an internal curing agent for mitigation of early-age cracking of high-performance concrete bridge decks. *Construction & Building Materials, 2011*, 25(1), 1-13. doi: 10.1016/j.conbuildmat.2010.06.063.
10. Ma X W., Liu J H., Shi C J. (2017): Effects of SAP on the properties and pore structure of high performance cement-based materials. *Construction and Building Materials, 131,* 475-484. doi: 10.1016/j.conbuildmat.2016.11.090.
11. Gupta S D. (2017): Combination of polypropylene fibre and superabsorbent polymer to improve physical properties of cement mortar. *Magazine of Concrete Research, 70*(7), 350-364. doi: 10.1680/jmacr.17.00193.
12. Shen D J., Wang X D., Cheng D B., et al. (2016): Effect of internal curing with super absorbent polymers on autogenous shrinkage of concrete at early age, *Construction and Building Materials, 106,* 512-522. doi: 10.1016/j.conbuildmat.2015.12.115.
13. Yao Y., Zhu Y., Yang Y Z. (2012): Incorporation superabsorbent polymer (SAP) particles engineered cementitious composites (ECC). *Construction and Building Materials, 28*(1), 139-145. doi: 10.1016/j.conbuildmat.2011.08.032.
14. Jensen O M., Hansen P F. (2002): Water-entrained cement-based materials. *Cement & Concrete Research, 32*(6), 973-978. doi: 10.1016/S0008-8846(02)00737-8.
15. Kong X M., Zhang Z L., Lu Z C. (2015): Effect of pre-soaked superabsorbent polymer on shrinkage of high-strength concrete, *Materials and structure, 48*(9), 2741-2758. doi: 10.1617/s11527-014-0351-2.
16. Lura P., Ye G., Cnude V., et al. (2006): Effects on material properties of self-compacting fibre-reinforced high performance concrete, *International RILEM proceedings, 52*, 87–96.
17. JC/T603-2004, Standard Test Method for Drying Shrinkage of Mortar. China Standard Publishing House, Beijing, China, 2004 (in Chinese). http://cx.spsp.gov.cn/.
18. GB/T 17671-1999: Testing Method of Cement Mortar Strength. China Standard Publishing House, Beijing, China,1999 (in Chinese). http://cx.spsp.gov.cn/.
19. Cuevas Karla., Lopez Mauricio. (2020): The effect of expansive agent and cooling rate in the performance of expanded glass lightweight aggregate as an internal curing agent. *Construction and Building Materials, 271*. doi:10.1016/J.CONBUILDMAT.2020.121505.
20. Benstend P., Basens P. (2009): The structure and performance of cement. Translated by Liao X. *Chemical Industry Press*, (in Chinese), *89*. ISBN:978-7-122-02991-1